Long-range order parameter of single $L1_0$-FePd nanoparticle determined by nanobeam electron diffraction: Particle size dependence of the order parameter

Kazuhisa Sato[a] and Yoshihiko Hirotsu
The Institute of Scientific and Industrial Research, Osaka University 8-1 Mihogaoka, Ibaraki, 567-0047 Osaka, Japan

Hirotaro Mori
Research Center for Ultra High Voltage Electron Microscopy, Osaka University Yamadaoka, Suita, 565-0871, Japan

Zhouguang Wang and Tsukasa Hirayama
Japan Fine Ceramics Center (JFCC), 2-4-1 Mutsuno, Atsuta-ku, Nagoya, 456-8587, Japan

(Received 14 March 2005; accepted 1 June 2005; published online 21 July 2005)

The long-range order (LRO) parameter (S) of single isolated $L1_0$-FePd nanoparticle was determined by quantitative analysis of nanobeam electron diffraction (NBD) intensities and intensity calculations considering the multiple scattering of electrons. The obtained order parameters of the nanoparticles larger than 8 nm are distributed around the mean LRO parameter ($\bar{S}=0.79$) which was determined by selected area electron diffraction intensity analysis, while the parameters slightly decreased gradually as the particle size decreased below about 8 nm ($S=0.60-0.73$). The low degree of order in very small particles is responsible for the coercivity decrease of the $L1_0$ nanoparticles in smaller-sized regions. Quantitative NBD intensity analysis is quite useful for the determination of the LRO parameter of individual $L1_0$-FePd single crystalline nanoparticle. Experimental conditions required for NBD analysis are presented in detail and the possible experimental errors of the determined LRO parameters are discussed. © *2005 American Institute of Physics*. [DOI: 10.1063/1.1985973]

I. INTRODUCTION

Hard magnetic properties of FePd nanoparticles with the $L1_0$-type structure are originated from large magnetocrystalline anisotropy constant (K_u).[1,2] The $L1_0$-type tetragonal ordered structure is known as the alternative stacking of Fe (001) and Pd (001) along the [001] direction. The $L1_0$-FePd nanoparticles with considerably small particle size act as single-domain particles, and their magnetization process is carried out by rotation magnetization. The [001] axis (c axis) of the $L1_0$ structure corresponds to the magnetic easy axis. Large K_u values of the $L1_0$-FePt as well as FePd nanoparticles resulted in an appearance of very large coercivity at room temperature even in 10-nm-sized small particles, which is suitable for ultra-high-density magnetic storage media.[3] Actually, K_u of these $L1_0$ alloys is ten times larger than that of the currently used CoCr-based recording media, which indicates a high thermal stability of magnetization in smaller-sized particles, leading to an increase of areal density. Moreover, large saturation magnetization of these $L1_0$ alloys as large as about 1100 emu/cm^3, which is three times larger than that of CoCr-based film, will ensure the high sensitivity in very thin and/or very small particle regions. Because of the above advantages, $L1_0$-FePt and FePd nanoparticles have been attracting much interest and have been studied extensively.[4] Recently, the authors have fabricated very small isolated $L1_0$-FePt particles with sizes less than 10 nm in diameter, where coercivity rapidly decreased with particle size reduction, especially below 8 nm (Ref. 5). The decrease of coercivity was also observed at 10 K where thermal fluctuation of magnetization is insignificant, indicating the decrease of the degree of long-range order or K_u in the very small particles. Although there has been reported a relation between K_u and the long-range order (LRO) parameter (S) in FePt thin films,[6,7] relations between K_u and particle size and between long-range order (LRO) parameter and particle size in the isolated $L1_0$ particles are still open questions. So it is important to know the LRO parameter of an individual $L1_0$ particle and its dependence on particle diameter in very small particle-size region. In order to determine the LRO parameter of a single $L1_0$ particle, we cannot use x-ray diffraction technique any longer. Recently, the authors have developed a method to determine the LRO parameter of an assembly of $L1_0$ particles with orientation by selected-area electron diffraction (SAED) with the aid of intensity calculations, considering the multiple scattering of electrons.[8,9] In these studies, 10-nm-sized FePt and FePd particles were epitaxially grown on NaCl (001) substrates and each particle was well isolated and separated by amorphous (a-) Al_2O_3 thin film. Therefore no phase relation exists, nor any double diffraction occurs among the particles, so we considered that the multiple scattering of electrons occurs within each particle in the intensity calculation. The above configuration of the $L1_0$ par-

[a]Electronic mail: sato@sanken.osaka-u.ac.jp

ticles makes quantitative diffraction intensity analyses easy when single crystalline particles are considered.

In the present study, we applied the above method using nanobeam electron diffraction to determine the LRO parameter of an individual $L1_0$-FePd nanoparticle, which leads to a clear particle size dependence of the LRO parameter. One-to-one correspondence between a LRO parameter and a particle size can be achieved in the present study, since we can obtain both a nanobeam electron diffraction (NBD) pattern and a particle image from the same particle using a transmission electron microscope (TEM). Also such parameters as the lattice parameter, the alloy composition, and the particle thickness, which are important factors in the LRO parameter determination, are all evaluated by TEM.

II. EXPERIMENT

Nanoparticles of FePd alloy were fabricated by successive deposition of Pd and Fe onto NaCl substrate cleaved in air.[10] The evaporation was performed by an electron-beam deposition apparatus operated at 4 kV with a base pressure of approximately 3×10^{-7} Pa. Pure Pd (99.95%), Fe (99.97%), and Al_2O_3 (99.99%) crystals were used as evaporation sources. The substrate temperature was kept at 673 K during the deposition of Pd and Fe. A quartz thickness monitor located near the substrate stage in the vacuum chamber was used to estimate the average thickness of the deposited layer. In the successive deposition process, Pd nanoparticles act as nucleation sites for Fe nanoparticles and formed Fe/Pd nanocomplex particles in the as-deposited condition, and nanoparticles are mutually separated by further successive deposition of a-Al_2O_3 film. The specimen film was removed from the NaCl substrate by immersing the substrate into distilled water, and was mounted onto copper grids for later TEM observation. Then annealing of the as-deposited specimen film on a copper grid was performed in a high-vacuum furnace ($<2\times10^{-5}$ Pa) at 873 K for 36 ks. The heating and the cooling rates were about 5 and 10 K/min, respectively. Structural characterization including NBD and SAED experiments were performed by TEM operated at 300 kV (JEOL JEM-3000F). SAED patterns were also observed using a high-voltage TEM operated at 1 MV (Hitachi H-3000). Images and diffraction patterns were recorded by using an imaging plates (IPs, Fuji Film FDL-UR-V) as digital data for later quantitative intensity analyses. In the reading process of electron intensities recorded in IPs, we took the fading effect of IP into consideration.[11] Averaged alloy composition of the fabricated nanoparticles was determined to be Fe–58 at. % Pd by energy dispersive x-ray spectroscopy (EDS). Specimen thickness was evaluated by electron holography using a biprism installed in the TEM (Hitachi HF-2000 and JEOL JEM-3000F). The electron probe size used in the NBD experiments was about 4 nm, which was determined by full-width at half maximum (FWHM) of the electron intensity profile, and a convergence angle of incident beam defined as a semicone angle was set to be about 4×10^{-4} rad in order to ensure the parallel beam illumination. In the present electron diffraction study, the ratio of the 110 superlattice and the 220 fundamental reflections was used to evaluate the S value of the $L1_0$-FePd nanoparticles. The intensity ratio I_{110}/I_{220} strongly depends on the film orientation in NBD. In taking NBD patterns, $hh0$ systematic reflections were excited using the 300-kV TEM.

TABLE I. Numerical parameters used for multislice calculations.

Alloy composition	Fe–58 at. % Pd	
Lattice parameter	a=0.383 nm, c=0.366 nm	
Zone axis	$[\bar{1}14]$, $[\bar{1}16]$, $[\bar{1}18]$	
Debye-Waller factor	0.0035 nm^2 (Fe), 0.0045 nm^2 (Pd)	
Spatial frequency limit	30 nm^{-1}	
Accelerating voltage	300 kV	1 MV
Slice thickness	0.14 nm	0.28 nm
Absorption (Imaginary potential)	10% of Real potential	

Transmitted and diffracted beam intensities were calculated based on the multislice method[12] using a computer software, MACTEMPAS PPC. The $L1_0$ structure belongs to the space group of $P4/mmm$, which gives the following structure factors of reflection: $F_{hkl}=4(x_{Fe}f_{Fe}+x_{Pd}f_{Pd})$ for hkl unmixed (all even or all odd) and $F_{hkl}=2|f_{Fe}-f_{Pd}|$ for hkl mixed. A slight beam tilting from the [001] incidence towards the $[\bar{1}10]$ direction results in an excitation of $hh0$ systematic reflections, which reduces diffracted beams and can largely decrease and simplify the multiple scattering events among the transmitted and the diffracted waves.[8,9] According to the multislice calculations, the intensity ratio, I_{110}/I_{220}, shows an oscillation with specimen thickness under the [001] incidence even for very thin regions below 15-nm thick, while in the case of $[\bar{1}14]$, $[\bar{1}16]$, and $[\bar{1}18]$ incidences, the intensity ratio increases monotonically with thickness.[8,9] In the following intensity analysis of NBD patterns, we deal with the beam incidences of $[\bar{1}14]$, $[\bar{1}16]$, and $[\bar{1}18]$, and weak reflections other than the $hh0$ systematic reflections are also taken into consideration. Reflection intensities with scattering vectors ($\equiv\sin\theta/\lambda$) up to 30 nm^{-1} were taken in the calculation, which is enough spatial frequency to calculate the diffracted intensities correctly.

The degree of order was changed by varying the atom fractions of sublattices of the $L1_0$ structure in the calculation using the following definition[13] of the order parameter:

$$S=\frac{r_\alpha-x_A}{y_\beta}=\frac{r_\beta-x_B}{y_\alpha}, \tag{1}$$

where $r_\alpha(r_\beta)$, $x_A(x_B)$, and $y_\alpha(y_\beta)$ denote the fraction of α sites (β sites) occupied by the right atoms, the atom fraction of A atoms (B atoms) represented by averaged alloy composition (in this study, x_A=0.42, A denotes Fe), and the fractions of α sites (β-sites), respectively. Numerical parameters used in the calculation are listed in Table I, where lattice parameters of FePd nanoparticles were determined by SAED using Pt polycrystalline thin film as an internal standard.[9] The accurate value of the temperature factor (Debye-Waller factor, B) for 10-nm-sized FePd nanoparticles is not known,

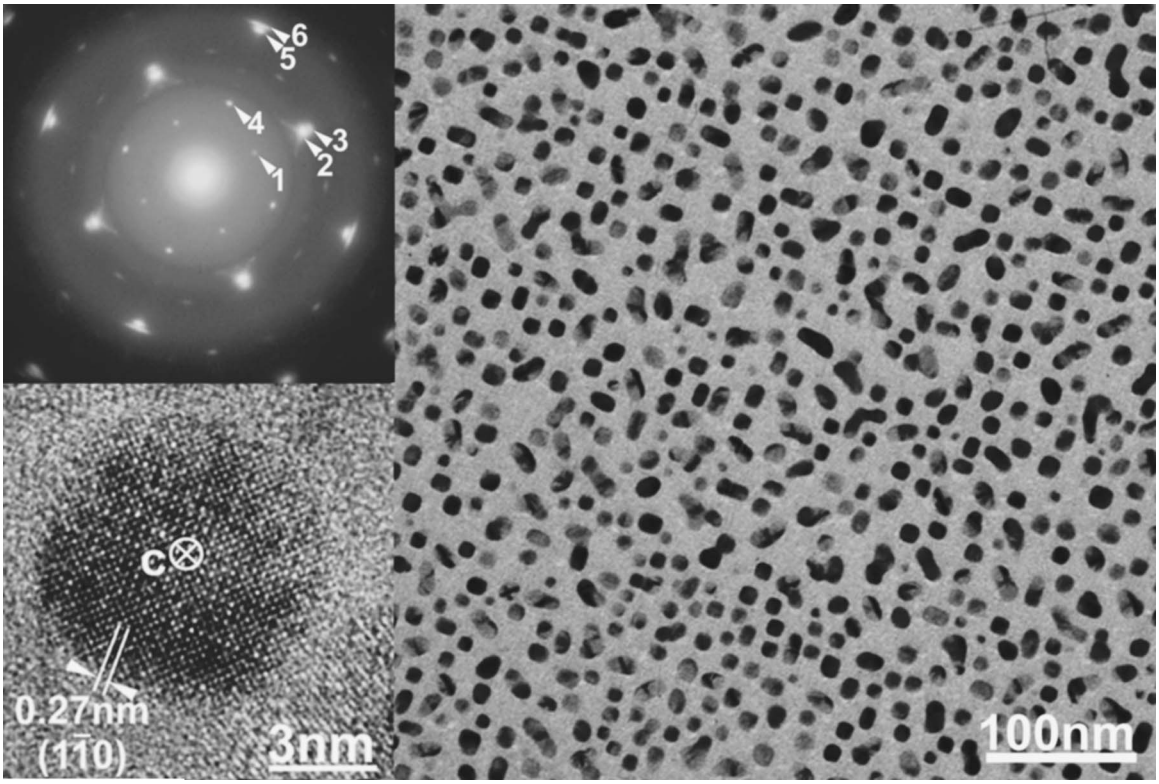

FIG. 1. A BF-TEM image and the corresponding SAED pattern for $L1_0$-FePd nanoparticles after annealing at 873 K for 36 ks. Small nanoparticles as small as 10 nm are finely distributed with mutual fixed orientation. A HREM image of a 7-nm-sized FePd nanoparticle is also shown in inset. Indices of reflections marked by arrows in the attached SAED pattern are as follows: (1) 001_{FePd}, (2) 200_{FePd}, (3) 002_{FePd}, (4) 110_{FePd}, (5) 220_{FePd}, and (6) 202_{FePd}. Reflections of 001, 002, and 202 come from the FePd nanoparticles with *c* axes oriented parallel to the film plane.

so we took $B=0.0035$ and 0.0045 nm^2 for Fe and Pd, respectively, after the values for bulk metals.[14]

III. RESULTS AND DISCUSSION

A. Nanoparticle morphology and compositions

A bright-field (BF) TEM image and the corresponding SAED pattern for $L1_0$-FePd nanoparticles fabricated by our technique are shown in Fig. 1. Nanoparticles as small as 10 nm are uniformly dispersed, and also *c* axes of the FePd nanoparticles are oriented both normal and parallel to the film plane as shown in the SAED pattern. A high-resolution TEM (HREM) image with the [001] orientation is shown in the lower inset. Clear {110} lattice fringes of the $L1_0$ structure is seen even in a 7-nm-sized small nanoparticles. The particle diameter distribution followed a log-normal-type distribution function with a mean diameter and a standard deviation of 11 nm and $\ln \sigma = 0.21$, respectively. Since these $L1_0$-FePd nanoparticles were epitaxially grown on the substrate with orientation, all the particles are oriented with their *c* axes normal or parallel to the *a*-Al_2O_3 film plane, which was revealed by SAED and HREM observations.[10] It was also confirmed that the population of FePd nanoparticles with their *c* axes oriented normal to the film plane were larger in number than those with *c* axes parallel to the film plane. Nanoparticles with crystallographic variant domains composed of more than two crystalline domains with orthogonal *c* axes were few in number.[10] These islandlike nanoparticles are distributed two dimensionally on the *a*-Al_2O_3 film. Since there is no overlapping of particles along the electron-beam direction when we observed the specimen in the plan-view condition, no double diffraction occurs between the isolated islands. The multiple scattering only occurs within each nanoparticle during the propagation of electrons. All these specimen conditions are convenient for quantitative analyses of electron diffraction intensities in this study.

The LRO parameter depends on the alloy composition as shown in Eq. (1), so it is necessary to know the composition distribution from particle to particle before the LRO parameter determination from single isolated FePd nanoparticle. A series of compositional analyses from nanoparticles to nanoparticles was performed using nanobeam EDS with a probe size of approximately 5 nm in diameter. In the analyses, the specimen film was tilted 10° towards the EDS detector in order to enhance the detection efficiency. Figure 2 shows a histogram of alloy composition of the present specimen. Although a distribution of alloy compositions is observed, the distribution is narrow with a standard deviation of 4 at. % Pd. We also examined a particle diameter dependence of the alloy composition by NBD together with BF image observation of the FePd nanoparticles. As a result, it was found that the alloy composition of the present FePd nanoparticles was almost independent of the particle diameter as shown in Fig. 3 in the particle size range between 6.5 and 17 nm. The presently analyzed particle diameter range almost corresponds to the range of the diameter distribution.[10]

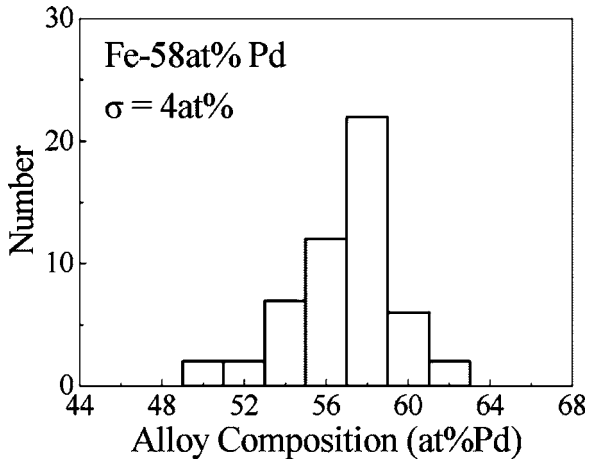

FIG. 2. A histogram of the alloy composition of FePd nanoparticles analyzed by nanobeam EDS. The mean composition was 58 at. % Pd with standard deviation of 4 at. %. The population of particles with mean composition was 41.5%.

B. Thickness dependence of the I_{110}/I_{220} intensity ratio

Because of the multiple scattering of electrons as well as the absorption effect, transmitted and diffracted beam intensities vary with specimen thickness complicatedly.[12] The thickness dependences of diffraction intensities were calculated by multislice method.[12] As explained in Sec. II, we took the tilted-beam conditions to excite *hh*0 systematic reflections to reduce the complex change of intensities with thickness. The number of waves of 91, 69, and 43 were taken in the calculation under the beam incidence of $[\bar{1}14]$, $[\bar{1}16]$, and $[\bar{1}18]$, respectively. The imaginary part of the projected potential was set to be 10% of the real part in order to consider the absorption effect of electrons within the specimen. Figure 4 shows the calculated thickness dependence of the intensity ratio I_{110}/I_{220} as a function of the LRO parameter, where 110 and 220 denote the superlattice and the fundamental reflections, respectively. The intensity ratios rapidly increase with thickness and this tendency is prominent in the higher degrees of order. The relation between the intensity ratio and the thickness shown in Fig. 4 is the basis for the LRO parameter determination by NBD from single crystalline nanoparticles.

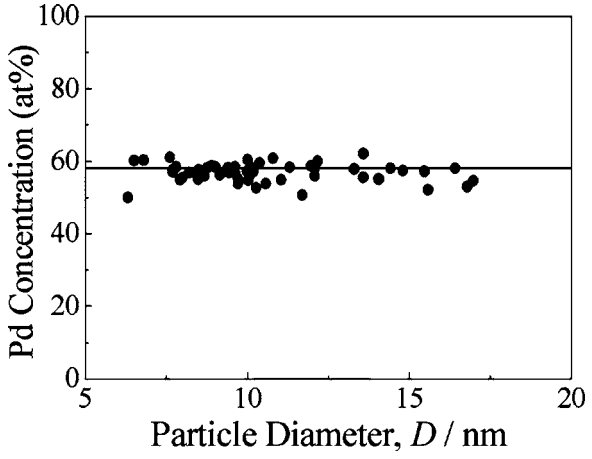

FIG. 3. Particle diameter dependence of the alloy composition for FePd nanoparticles analyzed by nanobeam EDS and the corresponding BF images. Alloy composition is independent of the particle diameter. The solid line indicates the mean alloy composition of Fe-58 at. % Pd.

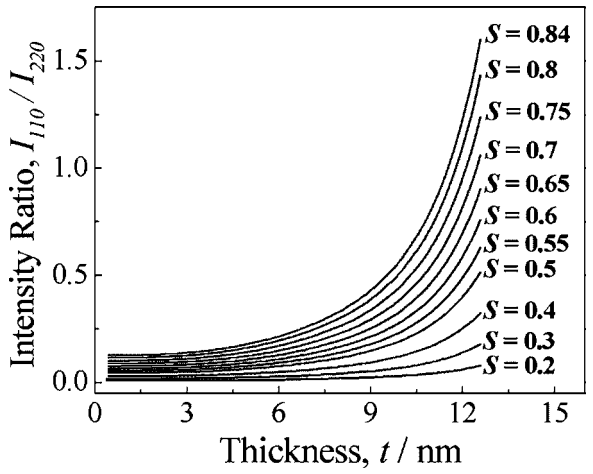

FIG. 4. Thickness dependence of the calculated intensity ratio I_{110}/I_{220} for 300-kV electrons under several degree of order. The order parameter was changed by varying the atom fractions of sublattices in the calculation. The beam incidence is $[\bar{1}16]$.

C. Evaluation of mean inner potential for the determination of particle thickness

For the determination of the LRO parameter of an isolated nanoparticle by NBD, it is necessary to know the correct thickness value of the particle. For this purpose, we took advantage of electron holography from which the thickness of each nanoparticle can be evaluated. For the correct evaluation of the thickness, the mean inner potential of the $L1_0$-FePd must be properly known. In the following, we at first determine the specimen thickness (t) before derivation of the LRO parameters for each FePd nanoparticle using NBD. In the electron holography, specimen thickness change and the mean inner potential are related based on the following equation:[15,16]

$$\Delta t \equiv \frac{2E_0\lambda}{V_0}\frac{1+(eE_0/2m_0c^2)}{1+(eE_0/m_0c^2)}, \tag{2}$$

where Δt denotes the thickness change, E_0 the accelerating voltage, m_0 the rest mass of electron, λ the electron wave length, and V_0 the mean inner potential.

Before the thickness determination of each FePd nanoparticles, we estimated the mean inner potential of 10-nm-sized FePd nanoparticles using the mean thickness which was determined by another method. For this purpose, we introduced a method to determine the average specimen thickness from the diffracted beam intensities using different accelerating voltages and then we derived the mean inner potential from Eq. (2) using the determined mean thickness. Relations between S and t shown in Fig. 5 were derived using the experimentally determined intensity ratios I_{110}/I_{220} of 0.293 and 0.141 obtained by SAED under 300 kV and 1 MV, respectively. That is, the curves shown in Fig. 5 indicate the possible combination of S and t under the experi-

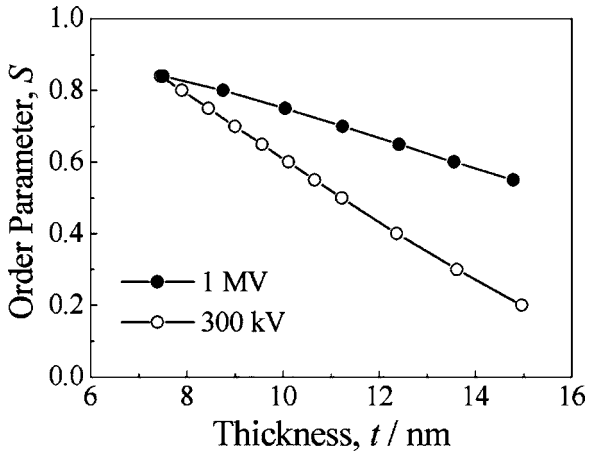

FIG. 5. Thickness dependence of the order parameter for 300-kV and 1-MV electrons derived based on the experimentally obtained intensity ratios with beam incidence of $[\bar{1}16]$.

mentally obtained I_{110}/I_{220} intensity ratios. From the cross point of these two curves the average thickness was obtained uniquely as $\bar{t}=7.6$ nm. Therefore, all parameters except for V_0 are already known since we determined the thickness from the cross point in Fig. 5. Using Eq. (2), the mean inner potential was determined to be 23.9 V for the 10-nm-sized isolated FePd nanoparticles with a mean thickness of 7.6 nm, which is 9.1% smaller than that theoretically derived (26.3 V, Ref. 9) based on the following equations:

$$V_0 = \left(\frac{h^2}{2\pi m_0 e}\right)\frac{1}{\nu_c}F(000), \tag{3}$$

$$F(000) = 4(x_{\mathrm{Fe}}f_{\mathrm{Fe}}(0) + x_{\mathrm{Pd}}f_{\mathrm{Pd}}(0)), \tag{4}$$

where h represents Plank's constant, e is the electron charge, ν_c is the volume of the unit cell, $f(0)$ is the atomic scattering factor for electrons at $\sin\theta/\lambda=0$ after the values by Rez *et al.*,[17] and $F(000)$ is the structure factor for the forward scattering of electrons. Then we measured the thicknesses of FePd nanoparticles from particle to particle by electron holography using the presently determined mean inner potential of 23.9 V. An example of electron hologram and its interferogram amplified 20 times are shown in Figs. 6(a) and 6(b), respectively. Straight interference fringes are observed in the electron hologram [Fig. 6(a)]. These fringes are due to the interference of two kinds of waves transmitted through vacuum and specimen. In the interferogram, contour fringes are observed within the particles. These contour fringes are due to the phase shift produced by the crystal potential change with the change of crystal thickness.[15,16,18] The process for the formation of an interferogram is explained elsewhere.[15,18] It should be noted that if the diffracted beam intensity is considerably strong compared with the transmitted wave, the phase change by diffraction is also overlapped with the above phase shift produced by crystal potential change.[16] So in the present electron hologram observation, the incident electron beam was set to be parallel to the [001] axis of FePd nanoparticles, where the intensity of the transmitted wave is much stronger than that of the diffracted waves. From the profiles of these fringes, it is found that all

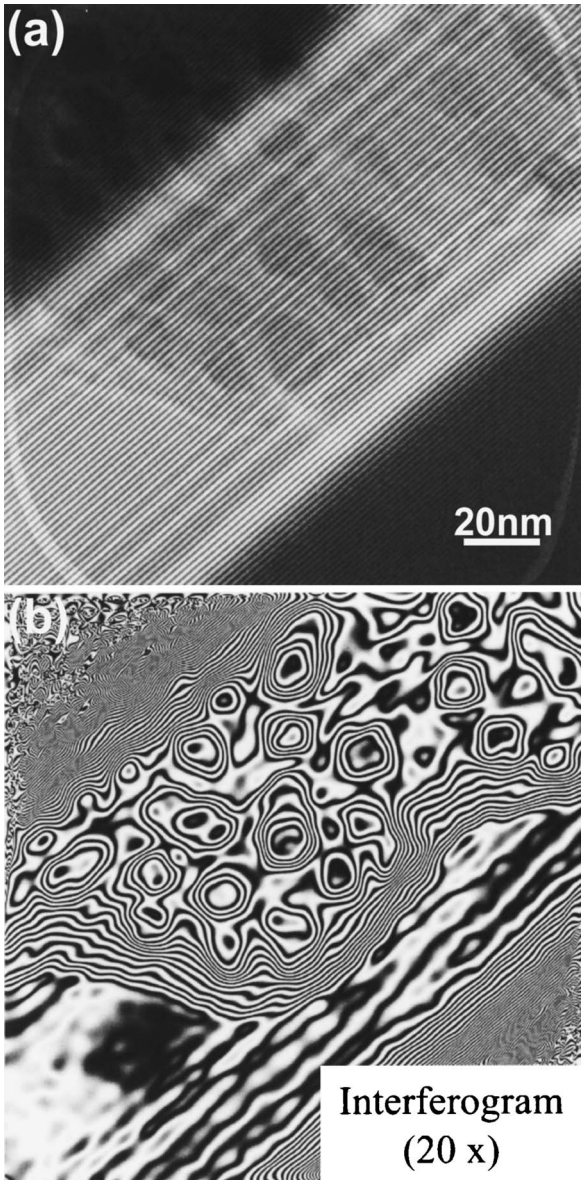

FIG. 6. (a) An electron hologram for FePd nanoparticles. (b) An interferogram corresponds to the electron hologram (amplification: ×20). The fringes due to the phase changes are clearly seen within the nanoparticles in the interferogram.

the FePd particles have flat top surfaces parallel to the substrate plane, and are almost pyramid-shaped with curved corners. As a result, we obtained a correlation between the particle diameter and the particle thickness as shown in Fig. 7, where particle diameter was determined by BF images corresponding to the interferogram. It was found that the particle thickness gradually increases with diameter without changing the pyramidal shape morphology, indicating the preferential particle growth towards the lateral direction on a flat NaCl substrate surface.

The cross point shown in Fig. 5 also indicates the mean order parameter $\bar{S}$ of 0.84. These $\bar{S}$ and $\bar{t}$ values which are determined independently by the accelerating voltages must be the real $\bar{S}$ and $\bar{t}$ values for the nanoparticles. Presently obtained these average $\bar{S}$ and $\bar{t}$ values are in quite good agreement with those evaluated in our previous study[9] using

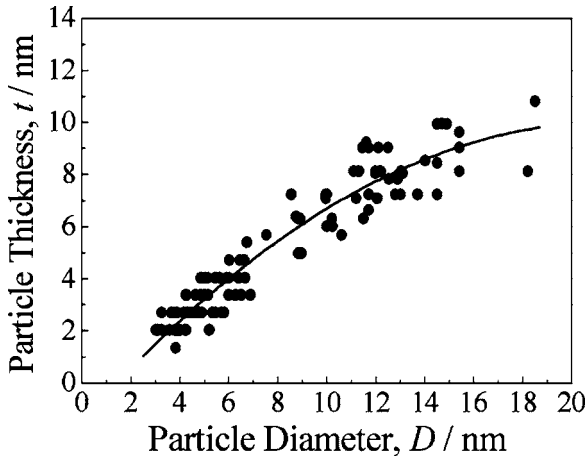

FIG. 7. Particle diameter dependence of the particle thickness for FePd nanoparticles measured by electron holography. The solid curve denotes the fitting of experimentally obtained data points. The mean deviation of data points from the fitting curve was 0.73 nm.

TEM and electron holography assuming the theoretical mean inner potential of 26.3 V, where the following parameters were derived: $\bar{S}=0.79$ and 0.82 for 300-kV and 1-MV cases, respectively, with $\bar{t}=7.8$ nm.

D. Determination of the LRO parameter of individual FePd nanoparticle

Figures 8(a)–8(d) show NBD patterns taken from FePd nanoparticles with diameters of 6.8, 8.2, 10.2, and 11.4 nm, respectively. The beam incidences were $[\bar{1}18]$ [Fig. 8(a)], $[\bar{1}14]$ [Figs. 8(b) and 8(d)], and $[\bar{1}16]$ [Fig. 8(c)]. The electron probe of about 4 nm in diameter was focused on the central region of each FePd nanoparticle in these NBD experiments. The intensity ratio I_{110}/I_{220} was measured from the intensity profile of these NBD patterns. In the NBD patterns obtained, we selected patterns almost satisfying the condition $I_{hkl}=I_{\overline{hkl}}$ for the correct order parameter determina-

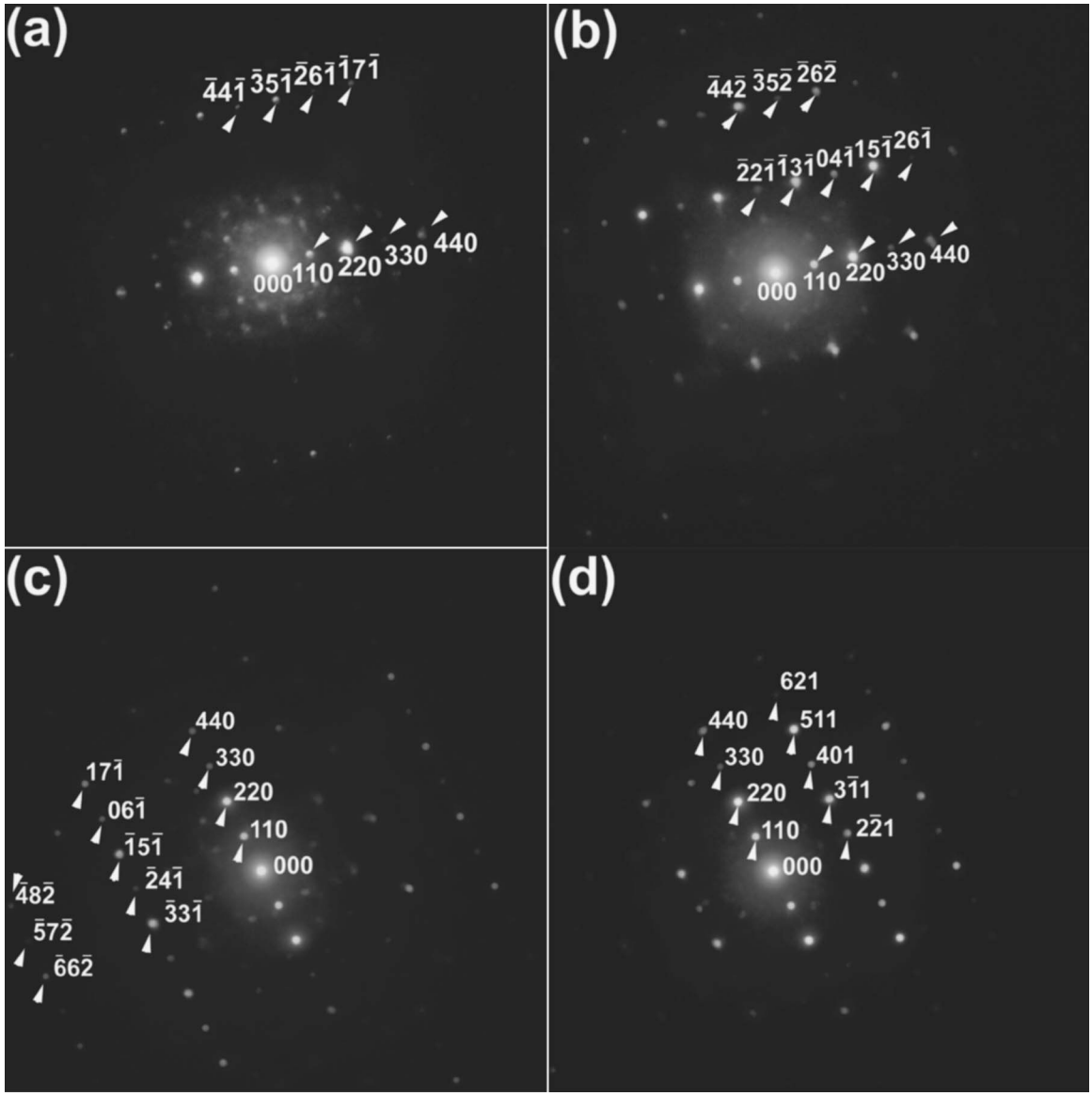

FIG. 8. NBD patterns for individual FePd nanoparticles observed at 300 kV. Particle diameter (D) and the beam incidence are as follows: (a) $D=6.8$ nm, $[\bar{1}18]$, (b) $D=8.2$ nm, $[\bar{1}14]$, (c) $D=10.2$ nm, $[\bar{1}16]$, and (d) $D=11.4$ nm, $[\bar{1}14]$.

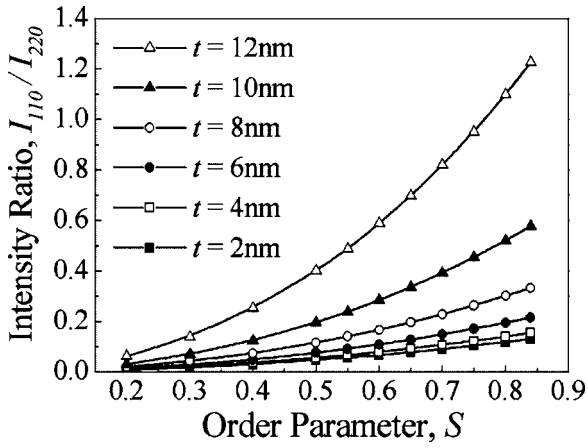

FIG. 9. Order parameter dependence of the I_{110}/I_{220} intensity ratio for several specimen thickness calculated by multislice method for 300-kV electrons. The LRO parameter can be derived from this viewgraph using the experimentally obtained intensity ratio when the specimen thickness is known.

tion. On the contrary, specimen tilt towards the $[\bar{1}10]$ direction does not affect the intensity ratio since the calculated intensity ratios under $[\bar{1}14]$, $[\bar{1}16]$, and $[\bar{1}18]$ beam incidences with different tilt angles exhibited an almost the same thickness dependence in the thickness range below 15 nm according to the intensity calculation.[9] On the basis of particle diameter determined by a BF image, the thickness of each particle for the NBD intensity analysis was determined using the relation shown in Fig. 7. The calculated relation between the intensity ratio and the LRO parameter is shown in Fig. 9 for several thicknesses, which was derived from the I_{110}/I_{220} thickness relation shown in Fig. 4. By comparing the experimentally obtained intensity ratio to the calculated one, the LRO parameter was determined uniquely. Figure 10 shows the particle size dependence of the LRO parameter of FePd determined by NBD intensity analyses. It was found that the LRO parameter slightly decreased with particle diameter reduction below about 8 nm. Order parameters expressed by open circles were obtained by assuming the mean alloy composition of Fe-58 at. % Pd since the distribution of the alloy composition is small. However, in order to make sure the alloy composition dependence of the LRO parameter, we also measured the alloy compositions from some particles by nanobeam EDS, in addition to the measurements of the NBD intensities and the particle sizes. These results are plotted by solid circles in Fig. 10. The lowest LRO parameter obtained in this study was $S=0.60$ for an FePd nanoparticle with a particle diameter of 7.1 nm. The alloy composition of this particle as measured by nanobeam EDS was Fe-58 at. % Pd, the same as the mean composition. Particles with alloy composition deviated from the mean composition also showed smaller LRO parameters than the averaged one when the particle diameter is smaller than about 8 nm. For example, $S=0.67$ was observed for Fe-55 at. % Pd nanoparticle with a diameter of 7.4 nm. The decrease of the LRO parameter with particle size reduction is again clearly shown regardless of the consideration of alloy composition of each FePd nanoparticle, indicating the fact that the observed decrease of the LRO parameter is essential for very small sized nanoparticles. The smallest particle analyzed in this study was 6.4 nm in diameter, which is close to the lower limit of the particle size distribution.[10] For more precise determination of the order parameter, it is necessary to clarify the particle size dependence of the Debye-Waller factors for Fe and Pd in isolated FePd nanoparticles. Actually, for example, the large increase of the Debye-Waller factors close to 0.01 nm^2 were reported for 2–3-nm-sized Cr,[19] Pd,[20] and Cu (Refs. 21 and 22) nanoparticles. However, it should be noted that consideration of the increase of the Debye-Waller factor due to a very small particle size resulted in a slight decrease of the LRO parameter at most 0.06 when $B=0.01$ nm^2 was assumed.[8,9] At this moment, the only remaining factor which may affect the LRO parameter is the distribution of the particle thickness. In the diameter-thickness curve shown in Fig. 7, the average thickness deviation of data points from the fitted curve was 0.73 nm, which resulted in a change of the LRO parameter of 0.07 for electron diffraction at 300 kV. On the contrary, the observed LRO parameter decreased to 0.60, which was much smaller than the mean LRO parameter of 0.79 determined by SAED at 300 kV. So it is concluded that the particle thickness distribution that exists in the present specimen gives an insignificant change of the LRO parameter. To check the electron irradiation effect on the $L1_0$ structure in the present NBD experiments, we observed the NBD pattern twice from the same particle. As a result, intensity profiles of these two NBD patterns perfectly overlapped each other and there was no significant difference among them. So it is concluded that there was no electron irradiation effect on the $L1_0$ structure in these NBD experiments.

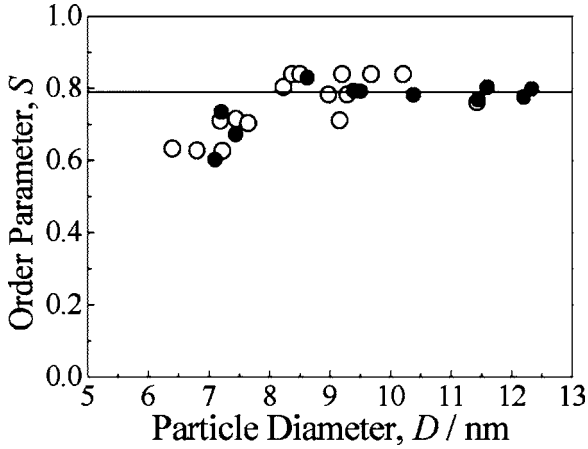

FIG. 10. Particle diameter dependence of the order parameter determined by NBD at 300 kV. The solid line indicates the mean LRO parameter determined by SAED at 300 kV. The LRO parameter slightly decreased with particle size reduction below 8 nm in diameter. For data points represented by solid circles, alloy composition of each FePd nanoparticle was analyzed by nanobeam EDS, while those of the open circles were determined assuming the mean alloy composition of Fe–58 at. % Pd.

Presently observed gradual decrease of the LRO parameter is a considerable reason for the decrease of coercivity of the $L1_0$ nanoparticles in very small sizes.[5] It is considered that the magnetocrystalline anisotropy constant is decreased due to the low degree of order in the small particle. From the structural viewpoint, the decrease of the LRO parameter with particle size reduction indicates an existence of the minimum

particle size for the $L1_0$ ordering. Actually, a formation of disorder Fe–Pd nanoparticles has been reported for 2-4-nm-sized isolated Fe–Pd nanoparticles based on HREM observations,[23] where very high temperature annealing as high as 920 K was performed before the HREM observations. Numerical calculations also indicate the existence of the size limit for the atomic ordering in isolated alloy nanoparticles.[24–26] The decrease of the Debye temperature is considered to cause the instability of ordered phase in small alloy nanoparticles,[27] but a relation between the gradual decrease of the order parameter and the Debye temperature is still an open question.

IV. CONCLUSION

The LRO parameter of single isolated $L1_0$-FePd nanoparticle has been determined by NBD and the multislice intensity calculation with the aid of thickness estimation by electron holography. In the analysis of electron hologram, the mean inner potential of 10-nm-sized FePd nanoparticles was evaluated to be 23.9 V, which was 9.1% smaller than that theoretically derived using atomic scattering factors for fast electrons. It was found that the LRO parameter of the FePd nanoparticle slightly decreases with particle size reduction below 8 nm in diameter. In this experiment, the alloy compositions of some of the particles were analyzed by nanobeam EDS just after the NBD observation in order to make sure the particle size dependence of the LRO parameter. Particle thickness distribution resulted in an insignificant change of the LRO parameter. It should be noted that the observed gradual decrease of the LRO parameter is considered to be a reason for the decrease of coercivity in very small sized $L1_0$ nanoparticles. A combination of quantitative NBD intensity analyses and the thickness determination by electron holography is quite useful for the determination of the LRO parameter of very small $L1_0$-FePd single crystalline nanoparticles. In order to get a precise quality of the determined order parameter, it is still necessary to clarify the particle size dependence of the Debye-Waller factors for Fe and Pd in isolated FePd nanoparticles when we get into the order parameter analysis in much smaller particle size regions less than 5 nm in diameter, where the temperature factors will significantly deviate from the corresponding bulk ones.

ACKNOWLEDGMENTS

This study was supported by the Grand-in-Aid for Scientific Research (S) (Grant No. 16106008), Grand-in-Aid for Young Scientists (B) (Grant Nos. 17760531 and 15760490), and Special Coordination Funds for Promoting Science and Technology on "Nanohetero metallic Materials" from the Ministry of Education, Culture, Sports, Science and Technology, Japan. This study was partly supported by Hosokawa Powder Technology Foundation.

[1] A. Kussmann and K. Müller, Z. Angew. Phys. **17**, 509 (1964).
[2] H. Shima, K. Oikawa, A. Fujita, K. Fukamichi, K. Ishida, and A. Sakuma, Phys. Rev. B **70**, 224408 (2004).
[3] D. Weller and M. F. Doerner, Annu. Rev. Mater. Sci. **30**, 611 (2000).
[4] For example, *Abstract of the Conference on $L1_0$ Ordered Intermetallic and Related Phases for Permanent Magnet and Recording Applications*, Copper Mountain, Colorado, August 15–20, 2004 (Engineering Conference International, Brooklyn, NY, 2004).
[5] K. Sato, T. Kajiwara, M. Fujiyoshi, M. Ishimaru, Y. Hirotsu, and T. Shinohara, J. Appl. Phys. **93**, 7414 (2003).
[6] H. Kanazawa, G. Lauhoff, and T. Suzuki, J. Appl. Phys. **87**, 6143 (2000).
[7] S. Okamoto, N. Kikuchi, O. Kitakami, T. Miyazaki, Y. Shimada, and K. Fukamichi, Phys. Rev. B **66**, 024413 (2002).
[8] K. Sato and Y. Hirotsu, Mater. Trans. **44**, 1518 (2003).
[9] K. Sato, Y. Hirotsu, H. Mori, Z. Wang, and T. Hirayama, J. Appl. Phys. **97**, 084301 (2005).
[10] K. Sato and Y. Hirotsu, J. Appl. Phys. **93**, 6291 (2003).
[11] T. Oikawa, D. Shindo, and K. Hiraga, J. Electron Microsc. **43**, 402 (1994).
[12] J. M. Cowley, *Diffraction Physics* 3rd ed. (Elsevier, Amsterdam, 1995), pp. 231–253.
[13] B. E. Warren, *X-ray Diffraction* (Dover, New York, 1990), pp. 208–210.
[14] N. M. Butt, J. Bashir, T. M. Willis, and G. Heger, Acta Crystallogr. **44**, 396 (1988).
[15] J. Endo, T. Matsuda, and A. Tonomura, Jpn. J. Appl. Phys. **18**, 2291 (1979).
[16] K. Yada, J. Crystallogr. Soc. Jpn. **17**, 226 (1975).
[17] D. Rez, P. Rez, and I. Grant, Acta Crystallogr. **50**, 481 (1994).
[18] A. Tonomura, T. Matsuda, T. Kawasaki, J. Endo, and N. Osakabe, Phys. Rev. Lett. **54**, 60 (1985).
[19] Y. Kashiwase, I. Nishida, Y. Kainuma, and K. Kimoto, J. Phys. Soc. Jpn. **38**, 899 (1975).
[20] K. Ohshima, S. Yatsuya, and J. Harada, J. Phys. Soc. Jpn. **50**, 3071 (1981).
[21] M. De Crescenzi, M. Diociaiuti, L. Lozzi, P. Picozzi, and S. Santucci, Phys. Rev. B **35** 5997 (1987).
[22] F.-W. Telgheder and J. Urban, J. Electron Spectrosc. Relat. Phenom. **95**, 267 (1998).
[23] H. Pan, S. Fukami, J. Yamasaki, and N. Tanaka, Mater. Trans. **44**, 2048 (2003).
[24] T. Tadaki, T. Kinoshita, Y. Nakata, T. Ohkubo, and Y. Hirotsu, Z. Phys. D: At., Mol. Clusters **40**, 493 (1997).
[25] Y. K. Takahashi, T. Koyama, M. Ohnuma, T. Ohkubo, and K. Hono, J. Appl. Phys. **95**, 2690 (2004).
[26] S. Fukami and N. Tanaka, Philos. Mag. Lett. **84**, 33 (2004).
[27] H. Yasuda and H. Mori, Z. Phys. D: At., Mol. Clusters **37**, 181 (1996).